Acoustical Physics, Vol. 49, No. 3, 2003, pp. 354–360. Translated from Akusticheskiĭ Zhurnal, Vol. 49, No. 3, 2003, pp. 416–424.

Reconstruction of the Normal Velocity Distribution on the Surface of an Ultrasonic Transducer from the Acoustic Pressure Measured on a Reference Surface

O. A. Sapozhnikov, Yu. A. Pishchal'nikov, and A. V. Morozov

Physics Faculty, Moscow State University, Moscow, 119992 Russia

e-mail: oleg@acs366.phys.msu.ru

Received May 8, 2002

Abstract—In piezoceramic ultrasonic transducers, the thickness vibrations are usually accompanied by the excitation of Lamb waves, which are difficult to control. Therefore, the normal velocity distribution over the radiating surface is unknown. As a result, the ultrasonic field generated by the transducer cannot be predicted with the desired accuracy. The purpose of this study is to develop and experimentally validate a new method for evaluating the normal velocity distribution over the surface of an ultrasonic transducer. The method consists in measuring the amplitude and phase of the acoustic pressure field over a certain reference surface and then calculating the acoustic field at the transducer by using the Rayleigh integral. The accuracy and stability of the method are illustrated numerically. The method is tested experimentally with a focused piezoceramic transducer. In the experiment, the reference surface is represented by a plane perpendicular to the axis of the acoustic beam. The ultrasonic field is scanned by a needle hydrophone, which is moved by a micropositioner. The measurements show that the method provides an accurate prediction of the acoustic field generated by a source with an unknown nonuniform normal velocity distribution. © *2003 MAIK "Nauka/Interperiodica"*.

INTRODUCTION

Piezoceramic transducers are widely used in visualization, ultrasonic therapy, nondestructive testing, and acoustic microscopy. To theoretically predict the acoustic fields they emit, it is necessary to know the normal velocity and acoustic pressure distributions on the radiating surface. The Rayleigh integral approximation [1], which represents the acoustic pressure at a given point in space as a superposition of spherical waves whose amplitudes are proportional to the normal velocity component at the corresponding points of the transducer, is most commonly used. For simplicity, it is usually assumed that the vibrations of a piezoceramic plate are determined by the thickness mode, i.e., that they are uniform over the radiating surface. However, the accuracy of this approximation is not very high, because the thickness vibrations of piezoceramic transducers are accompanied by other modes that are difficult to control, in particular, by the Lamb waves [2, 3]. Therefore, the distribution of the normal velocity over the transducer surface is nonuniform. It is difficult to theoretically predict the structure of the elastic vibrations of a piezoceramic plate, because the boundary conditions, which depend on the manner the plate is fixed to the body, and the electromechanical parameters of the piezoceramic material are known with a limited accuracy. At first sight, the optical interferometry method can be used to directly measure the normal velocity of the transducer surface vibrations. However, such measurements are only possible for a source operated in air. If the transducer operates in water, the acoustooptical interaction in the liquid plays a significant role. As a result, the signal from the interferometer cannot be explicitly related to the displacement of the surface [2]. Thus, the normal velocity (and, all the more so, the acoustic pressure) distribution over the piezoelectric transducer is actually unknown.

In this paper, we propose a method for reconstructing the normal velocity and the acoustic pressure on the surface of a transducer. The idea of the method is to use the time reversibility of the wave process [4]. The reconstruction procedure consists of two stages. First, the amplitude and phase of the wave is measured over a certain reference surface in front of the transducer. Second, the phase of the wave is reversed and the acoustic field is calculated numerically on the surface of the transducer by using the Rayleigh integral over the reference surface. Similar approaches were proposed earlier for calculating the acoustic fields produced by transducers. One of them represents the transducer as a multielement antenna array. The acoustic pressure measured experimentally at a number of points on the reference surface is expressed as a superposition of spherical waves produced by individual array elements and,

1063-7710/03/4903-0354$24.00 © 2003 MAIK "Nauka/Interperiodica"

then, the resultant system of linear algebraic equations is solved for the particle velocity on these elements [5]. The method has a clear limitation associated with the necessity to numerically solve systems of complex linear equations of a very high order. For example, if the pressure is measured over a 100×100 grid, the number of equations is 10000, which makes the solution of the problem by a personal computer actually impossible. The other method relies on the angular spectrum calculated from the parameters of the wave measured over the reference surface perpendicular to the acoustic axis. Theoretically, the field at other points in space can be calculated exactly from the angular spectrum and, in particular, the source distribution over an emitting surface can be reconstructed. In the practical realization, the accuracy of reconstructing the spatial source distribution can be limited by irregularities greater than the wavelength, because small-scale features of the distribution correspond to exponentially decaying (inhomogeneous) components of the angular spectrum. If the inhomogeneous waves are taken into account, the accuracy proves to be rather high. Such an approach is the basis of the so-called near-field acoustic holography [6–8]. Unfortunately, it is only applicable to comparatively low-frequency waves, for which the field can be measured at distances from the transducer that are smaller than or comparable to the wavelength. In the megahertz frequency range (medical applications and nondestructive testing), the distance between the measurement plane and the transducer is, as a rule, much longer than the wavelength. Therefore, the information on the high-frequency components of the angular spectrum is lost and, for the reconstruction algorithm to be stable, the inhomogeneous components of the spectrum must be set equal to zero [9–11]. As we noted above, this leads to a certain smoothing of the reconstructed distribution, as compared to the true one. A similar limitation is also inherent in the method considered in this paper. However, it should be noted that, unlike the angular spectrum method, the approach proposed below calculates a two-dimensional integral only once (the angular spectrum method performs the two-dimensional integration twice). In addition, in the phase reversal method, the surface over which the wave parameters are measured can be nonplanar. This advantage may be very useful in the studies of transducers that generate strongly divergent acoustic beams.

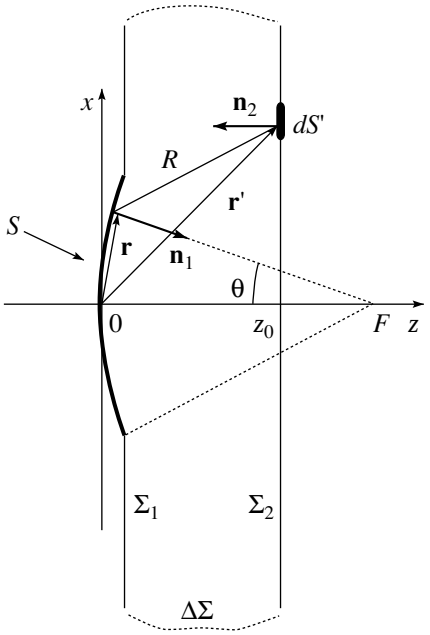

Fig. 1. Geometry of the problem.

THEORY

Consider an acoustic transducer built into a planar screen. Let the surface of the transducer with the screen be Σ_1 (Fig. 1), and let the acoustic pressure $p_2(\mathbf{r}, t)$ be measured on a plane surface Σ_2 that is parallel to the screen. The question arises of whether it is possible to reconstruct the acoustic field $p_1(\mathbf{r}, t)$ over the surface Σ_1 from the known distribution $p_2(\mathbf{r}, t)$. An affirmative answer to this question follows from the time reversibility of the wave process. In fact, the wave equation in a lossless medium, $\Delta p - c^{-2}\partial^2 p/\partial t^2 = 0$, does not change under the substitution $t \longrightarrow -t$. If the transducer is enclosed in a surface that is a perfect time-reversing (or, to put it differently, wave-front-reversing) mirror, the wave propagating to the transducer after the reflection from such a mirror completely reproduces its original parameters. As such a closed surface, we may take the surface consisting of Σ_1, Σ_2, and a side surface $\Delta\Sigma$ removed to infinity (see Fig. 1). However, the contribution due to $\Delta\Sigma$ vanishes, because the solid angle subtended by this surface tends to zero. The contribution of the surface Σ_1 can also be neglected, because the radiation in this direction is small. Hence, we can assume that, if the acoustic pressure on the plane Σ_2 is known, this data is sufficient to reconstruct the field on the transducer surface. The accuracy of the method is limited to about a wavelength; i.e., finer features are smoothed out. Indeed, the field reconstruction at a certain point on the transducer surface can be thought of as focusing of the phase-reversed field, so that the well-known diffraction limitation on the size of the focal spot necessarily manifests itself.

We restrict our analysis to a monochromatic source. In this case, the acoustic pressure can be represented as $p(\mathbf{r}, t) = |A|\cos(\omega t - \varphi) = (Ae^{-i\omega t} + A^* e^{i\omega t})/2$, where $|A|$ and φ are the wave amplitude and phase and ω is the circular frequency, so that $A(\mathbf{r}) = |A|e^{i\varphi}$ is the complex wave amplitude. We assume that the acoustic pressure on the reference plane Σ_2 is known from the measurements. If we mentally place a time-reversing mirror on Σ_2, the acoustic pressure in the reflected wave will have

the form $p(\mathbf{r}, -t) = (Ae^{i\omega t} + A^*e^{-i\omega t})/2 = (A_{\text{rev}}e^{-i\omega t} + A^*_{\text{rev}}\, e^{i\omega t})/2$; i.e., the amplitude of the time-reversed wave will be a complex conjugate of that of the incident wave: $A_{\text{rev}} = A^*$. To calculate the reflected wave on the left of Σ_2, we can use the Kirchhoff–Helmholtz integral, which represents the amplitude of the acoustic field emitted by a surface in terms of the normal velocity and acoustic pressure distributions over this surface. As is known, if the emitting surface is planar, the Kirchhoff–Helmholtz integral can be reduced to integrals that contain the distribution of either normal velocity or acoustic pressure alone [12]. In particular, if we use the acoustic pressure distribution, the Kirchhoff–Helmholtz integral has the form

$$A_{\text{rev}}(\mathbf{r}) = 2\int_{\Sigma_2} A_{\text{rev}}(\mathbf{r}')\frac{\partial G(\mathbf{r}, \mathbf{r}')}{\partial n_2(\mathbf{r}')}dS', \qquad (1)$$

where $G(\mathbf{r}, \mathbf{r}') = e^{ik|\mathbf{r}-\mathbf{r}'|}/4\pi|\mathbf{r}-\mathbf{r}'|$ is the Green's function of free space, k is the wave number, $\mathbf{n}_2(\mathbf{r}')$ is the unit outer normal to the surface Σ_2, and dS' is the element of this surface (Fig. 1). Since $A_{\text{rev}} = A^*$, we arrive at the expression for the original wave on the left of the plane Σ_2 in terms of the known wave amplitude distribution on Σ_2:

$$A(\mathbf{r}) = 2\int_{\Sigma_2} A(\mathbf{r}')\frac{\partial G^*(\mathbf{r}, \mathbf{r}')}{\partial n_2(\mathbf{r}')}dS'. \qquad (2)$$

With the position vector $\mathbf{r}$ placed on the surface Σ_1, this formula yields the unknown amplitude of the acoustic pressure on the transducer and the screen. To find the normal velocity component, we use the equation of motion. Let $V_n(\mathbf{r})$ be the complex amplitude of the normal component of the particle velocity $\mathbf{v}$. The equation of motion $\rho_0\partial\mathbf{v}/\partial t = -\nabla p$ yields $V_n(\mathbf{r}) = -(i/\omega\rho_0)\partial A/\partial n_1$, where ρ_0 is the density of the medium and $\mathbf{n}_1$ is the unit normal to the surface Σ_1. With Eq. (2), we have

$$V_n(\mathbf{r}) = -\frac{2i}{\omega\rho_0}\int_{\Sigma_2} A(\mathbf{r}')\frac{\partial^2 G^*(\mathbf{r}, \mathbf{r}')}{\partial n_1(\mathbf{r})\partial n_2(\mathbf{r}')}dS'. \qquad (3)$$

Expressions (2) and (3) constitute the theoretical basis of the method. As we can see, the acoustic pressure and the normal velocity component on the emitting surface can rather easily be reconstructed from the measured amplitude and phase distributions of the acoustic pressure over a certain reference surface Σ_2. Theoretically, the distance between the plane Σ_2 and the transducer can be arbitrary.

Note that formula (3) is derived under the assumption that the transducer is planar. For nonplanar transducers, an error associated with multiple reflections from the curved emitting surface takes place. However, for transducers with a small curvature and large wave dimensions of their surfaces, which are of interest in most applications, the error should be insignificant.

NUMERICAL MODELING OF A FOCUSED TRANSDUCER

In view of the experiment described in the following section, we consider an acoustic transducer in the form of a spherical bowl (surface S in Fig. 1). Such concave piezoelectric plates are widely used to produce focused ultrasonic beams in medical applications and in nondestructive testing. Due to the axial symmetry of the transducer, there is no need in measuring the amplitude and phase over the entire plane Σ_2. It is sufficient to perform one-dimensional measurements along the radius.

We consider only the normal velocity component on the transducer surface. Introducing the notation

$$K(\mathbf{r}, \mathbf{r}') = -\frac{2i}{\omega\rho_0}\frac{\partial^2 G^*(\mathbf{r}, \mathbf{r}')}{\partial n_1(\mathbf{r})\partial n_2(\mathbf{r}')}, \qquad (4)$$

we represent Eq. (3) in the form

$$V_n(\mathbf{r}) = \int_{\Sigma_2} A(\mathbf{r}')K(\mathbf{r}, \mathbf{r}')dS'. \qquad (5)$$

Here, A is the measured complex amplitude of the sinusoidal wave in the plane Σ_2. Let us make use of the axial symmetry of the problem. We characterize the position of the observation point on the spherical surface of the transducer by the angle θ between the symmetry axis and the straight line that passes through the observation point and the center of curvature of the transducer surface. To calculate integral (5), we introduce the polar coordinates (ξ, ψ) on the Σ_2 plane: $\mathbf{r}' = (\xi\cos\psi, \xi\sin\psi, z_0)$. Calculating the derivatives that enter into Eq. (4) along the normals by taking into account their directions (Fig. 1), we arrive at the following expression for kernel (4):

$$K(\mathbf{r}, \mathbf{r}') = \tilde{K}(\xi, \psi, \theta)$$
$$= -\frac{i}{\omega\rho_0}\frac{e^{-ikR}}{2\pi}\left\{(3\gamma + \cos\theta)\left(\frac{1}{R^3} + \frac{ik}{R^2}\right) - \gamma\frac{k^2}{R}\right\}, \qquad (6)$$

where

$$R = \{F^2 + \xi^2 + (F - z_0)^2$$
$$- 2F\xi\sin\theta\cos\psi - 2F(F - z_0)\cos\theta\}^{1/2}$$

is the distance between the observation point $\mathbf{r}$ and the point $\mathbf{r}'$ on the surface and $\gamma = [F(1 - \cos\theta) - z_0][F - \xi\sin\theta\cos\psi - (F - z_0)\cos\theta]/R^2$. The reference plane Σ_2 is at the distance z_0 from the center of the transducer,

and the center of curvature of the emitting surface, at the distance F (Fig. 1). Integral (5) takes the form

$$V_n(\theta) = \int_0^{2\pi} d\psi \int_0^{\xi_{\max}} \tilde{K}(\xi, \psi, \theta) A(\xi) \xi d\xi, \qquad (5a)$$

where $V_n(\theta)$ is the amplitude of the normal velocity on the transducer surface at the points corresponding to the angle θ, $A(\xi)$ is the pressure amplitude on the reference plane at the distance ξ from the symmetry axis, and $\xi_{\max}$ is the radius of the measurement region. The functions V_n and A depend on one variable each because of the axial symmetry. Integral (5a) can be calculated approximately as a sum over small surface elements of nearly the same area into which the circular measurement region of radius $\xi_{\max}$ is divided.

When implementing this method in practice, a number of questions arise, in particular, the questions of where is the best place for the reference plane; how wide the limits should be, where the field is measured on the reference plane, and what the step size should be; how does the error in the sound velocity affect the reconstruction accuracy; etc. To answer these questions, we used mathematical simulations. We studied a focused monochromatic transducer. Using the Rayleigh integral [13]

$$A(\mathbf{r}') = -i\frac{\rho_0 \omega}{2\pi} \int_{\Sigma_1} \frac{V_n(\mathbf{r}) e^{ik|\mathbf{r}-\mathbf{r}'|}}{|\mathbf{r}-\mathbf{r}'|} dS, \qquad (7)$$

we numerically calculated the acoustic pressure amplitude $A(\mathbf{r}')$ at different points of the reference plane. The initial normal velocity distribution was taken to be uniform: $V_n(\mathbf{r}) = 1$. Assuming that the calculated data $A(\mathbf{r}')$ represent some experiment, we used formula (5) to reconstruct the normal velocity distribution on the transducer surface. The result was compared with the initial (uniform) distribution $V_n(\mathbf{r})$.

Figure 2 shows the amplitude and phase of the velocity $V_n(\mathbf{r})$ on the transducer surface that were reconstructed for different positions of the reference plane. The horizontal axis represents the angle θ at which the points on the transducer surface are seen (θ = 0° corresponds to the center of the transducer, and θ = 14°, to its edge). The calculations were performed with the same parameters as the experiment described in the next section: the ultrasonic frequency was f = 1.1 MHz, the velocity of sound was c_0 = 1476 m/s, the radius of the measurement region was $\xi_{\max}$ = 6 cm, the transducer diameter was 10 cm, the transducer surface curvature radius was F = 22 cm, and the measurement step was 0.3 mm. As we see from this figure, the position of the reference plane, in which the acoustic pressure is measured, actually does not affect the reconstructed normal velocity.

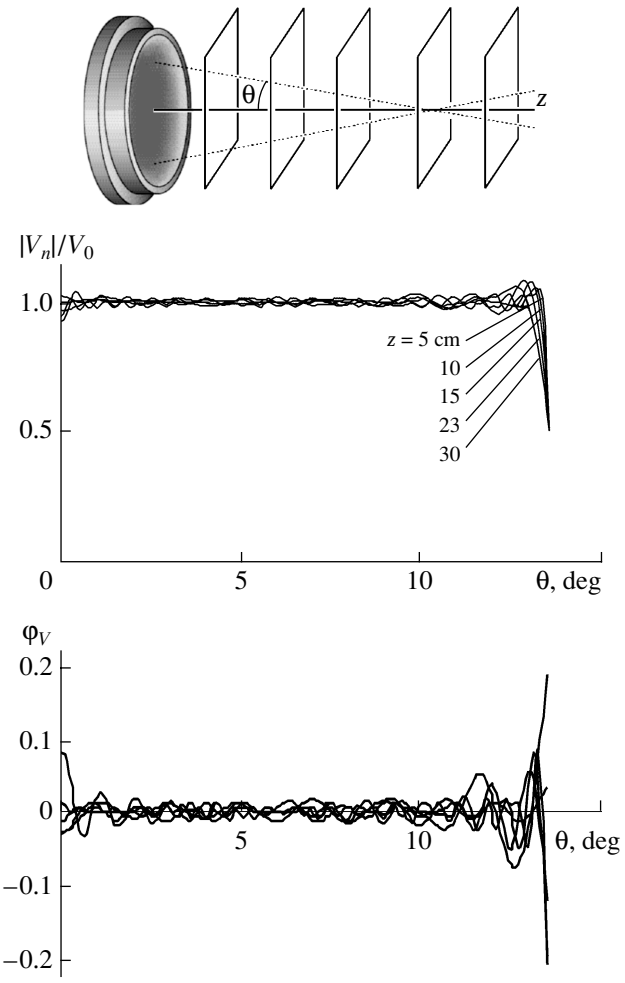

Fig. 2. Reconstruction of the normalized amplitude $|V_n|/V_0$ and phase φ_V (in radians) of the normal velocity on the transducer surface for different distances between the reference plane and the transducer: z_0 = 5, 10, 15, 23, and 30 cm; the horizontal axis represents the angle at which the points of the transducer surface are seen from the focal point: θ = 0° corresponds to the center of the transducer, and θ = 14°, to its edge.

Another source of error in the reconstructed distribution $V_n(\mathbf{r})$ may be an error in the value of the sound velocity. We estimated this effect on the accuracy of the method through the appropriate numerical modeling. As we described above, we calculated the field distribution in the reference plane from the Rayleigh integral under the assumption that the particle velocity distribution over the transducer surface is uniform. This "measured" distribution of the complex pressure amplitude was used to reconstruct the velocity at the transducer surface from formula (5) with another, perturbed, sound velocity value. Figure 3 presents the normal velocity reconstructed with the error Δc = 25 m/s introduced into the velocity of sound, which corresponds to a 10°C variation in the water temperature. For the sake

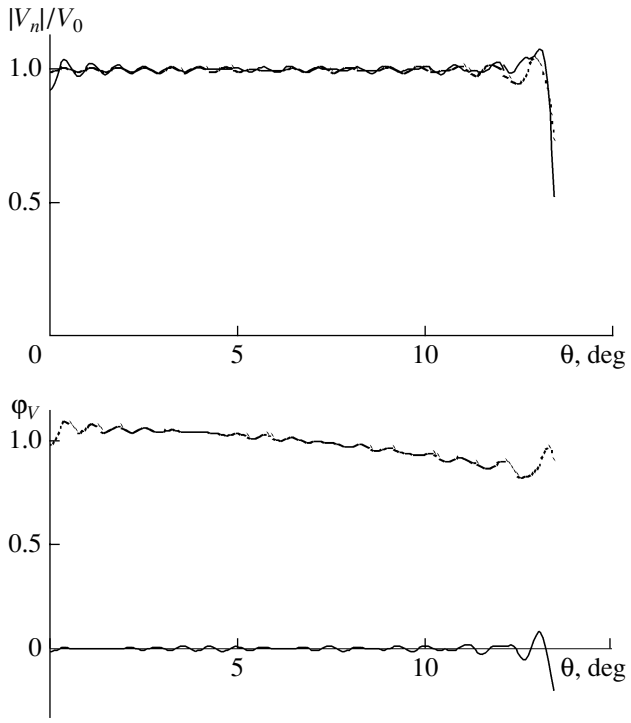

Fig. 3. Effect of the error Δc = 25 m/s introduced into the velocity of sound c_0 = 1476 m/s (which corresponds to a 10°C variation in the water temperature) on the normalized amplitude $|V_n|/V_0$ and phase φ_V (in radians) distributions of the normal velocity over the transducer surface.

of comparison, the dotted line shows the result of reconstruction for the unperturbed velocity of sound c_0 = 1476 m/s. Since the velocity of sound has changed, the phase acquires a certain shift. However, the initial uniform velocity amplitude distribution proves to be almost insensitive to the variation in the velocity of sound and is reconstructed with a sufficiently high accuracy.

EXPERIMENT

A concave piezoceramic transducer with a curvature radius F = 22 cm, a diameter of 10 cm, and a resonance frequency of 1.1 MHz was placed into a $60 \times 24 \times 30$-cm dish filled with settled tap water. The acoustic pressure was measured with a PVDFZ44-0400 SEA needle hydrophone with a sensitive region of 0.4 mm in diameter. After a preamplification, the hydrophone signal was recorded with a 520A Textronix digital oscilloscope. The hydrophone could be moved in three orthogonal directions with an accuracy of 0.01 mm by a Velmex-Unislide micropositioning system. A computer, which ran programs from the National Instruments (Austin, Tex.) in LabView language, was used to control the micropositioner and to read the signals from the oscilloscope. To avoid the effect of reverberation, the measurements used the pulsed operating mode. A rectangular high-frequency electric pulse was supplied to the transducer from an HP 33120A signal source. To model the operation in the CW mode, the pulse duration and the measurement time window were chosen so that the transient processes in the transducer and the hydrophone would be terminated while the signals reflected from the hydrophone body, the walls of the dish, etc. would not yet be received.

The experiment was conducted as follows. At first, we found the position of the symmetry axis (the 0z axis in Fig. 1), whose direction generally coincided with none of the micropositioner axes. To this end, the acoustic pressure amplitude distribution was measured at a certain distance from the transducer in a plane that was approximately orthogonal to the transducer axis. Based on these measurements, the program plotted the equiamplitude lines on the computer screen. They had the form of concentric circles with the center assumably lying on the symmetry axis of the transducer. Then, the hydrophone was placed at this point (center), and the time delay in the signal arrival was measured. After that, the hydrophone was moved a certain distance away from the transducer and the measurement procedure was repeated to determine the second point lying on the axis and to measure the delay in the signal arrival. The coordinates of the two points uniquely determined the symmetry axis, while the velocity of sound in water was calculated from the two delays and the distance between the points. Subsequently, special programs were used to measure the field in the plane orthogonal to the symmetry axis determined above. One of the resulting amplitude and phase distributions of acoustic pressure is shown in Fig. 4. The two-dimensional (upper) images illustrate the amplitude (on the left) and phase (on the right) distributions of acoustic pressure. The phase was measured relative to the signal fed to the transducer from the oscillator. As we see from these distributions, the axial symmetry of the acoustic field is quite pronounced. This means that the time taken to perform the experiment can be considerably reduced using the one-dimensional scan in any direction orthogonal to the symmetry axis instead of the two-dimensional scan. The corresponding one-dimensional amplitude and phase distributions are presented in the lower part of Fig. 4.

After the transverse amplitude and phase distributions of acoustic pressure were measured, the corresponding complex amplitude distribution of the field in the reference plane was calculated. Following the method proposed above, we used Eqs. (5a) and (6) to numerically reconstruct the distribution of the complex amplitude of the velocity over the transducer surface. Figure 5 shows the result of the reconstruction in the form of the dependences of the amplitude and phase of the normal particle velocity component on the angle θ. The acoustic pressure was measured at a distance z_0 =

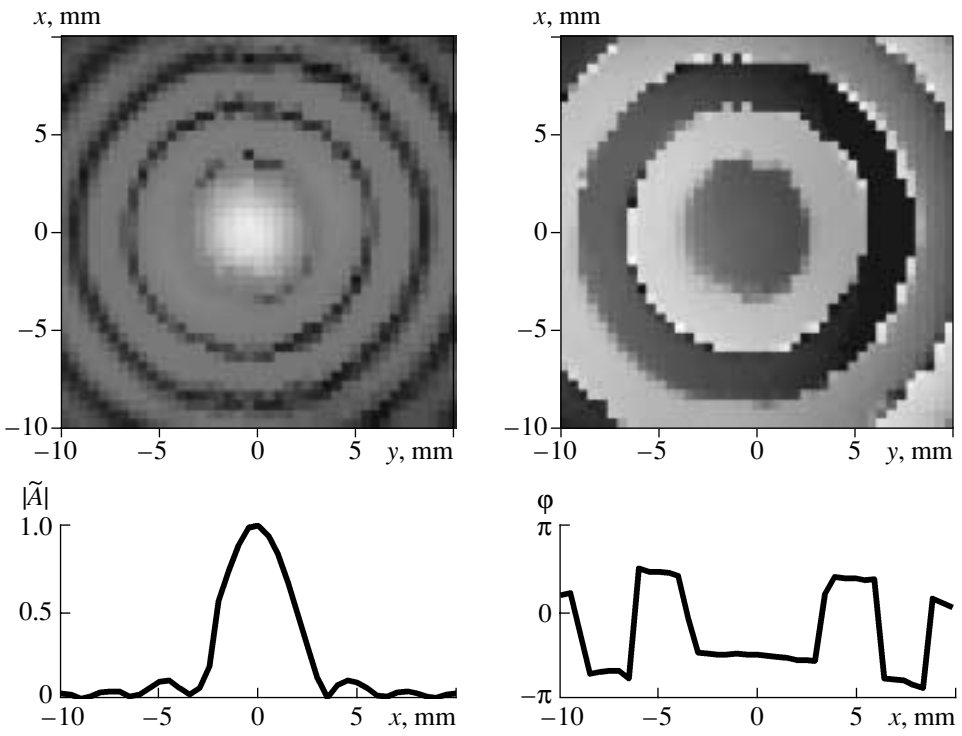

Fig. 4. Measured distributions of the normalized amplitude $|\tilde{A}| = |A|/A_0$ and phase φ of the acoustic pressure in the focal plane z = 220 mm. The upper panels show the two-dimensional distributions in the (x, y) coordinates represented as shades of gray with higher values corresponding to lighter shades. The point $(x, y) = (0, 0)$ corresponds to the hydrophone position on the transducer axis. The lower panels show the one-dimensional amplitude and phase (in radians) distributions along the transverse x axis.

214 mm from the transducer. One can see that the reconstructed amplitude and phase distributions of the particle velocity are nonuniform. They exhibit pronounced maxima and minima associated with the Lamb waves in the piezoceramic plate [2]. In particular, the velocity amplitude maximum at the center of the transducer (θ = 0°) is almost twice as high as the average amplitude of the particle velocity. For comparison, the thin line illustrates the numerical simulation under the assumption that the initial velocity distribution is uniform (see the previous section).

Note that the velocity reconstruction from the acoustic pressure measured at different distances from the transducer gives the same results. Figure 6 shows the normal velocity distributions reconstructed from the pressure measured at z_0 = 136, 165, and 214 mm. The plots demonstrate a qualitatively similar behavior; in particular, the positions and amplitudes of their maxima and minima almost coincide. Minor differences occur, because real transducers are not exactly axially symmetric and, in the general case, the reconstruction procedure should use the acoustic pressure measured over the entire plane rather than along a single line.

Using Rayleigh integral (7) and the reconstructed normal velocity on the transducer surface, one can calculate the acoustic field at any point of space. The comparison of this field with the field measured experimen-

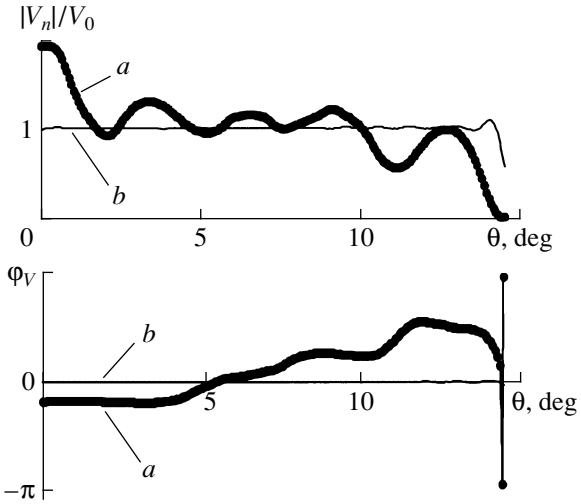

Fig. 5. Reconstruction of the normalized amplitude $|V_n|/V_0$ and phase φ_V distributions of the particle velocity over the transducer surface from the acoustic pressure measured along the transverse x axis at the distance z_0 = 214 mm from the transducer (curves *a*). The thin lines (curves *b*) show the distributions reconstructed from the theoretical pressure distributions created by a piston transducer at this distance. The angle θ = 0° corresponds to the center of the transducer, and the angle θ = 14°, to its edge.

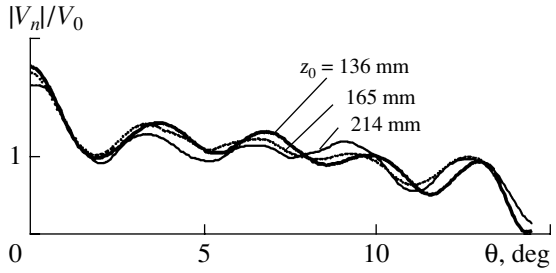

Fig. 6. Reconstruction of the velocity distributions over the transducer surface from the pressure measured along the normal to the acoustic axis at the distances z_0 = 136, 165, and 214 mm from the transducer.

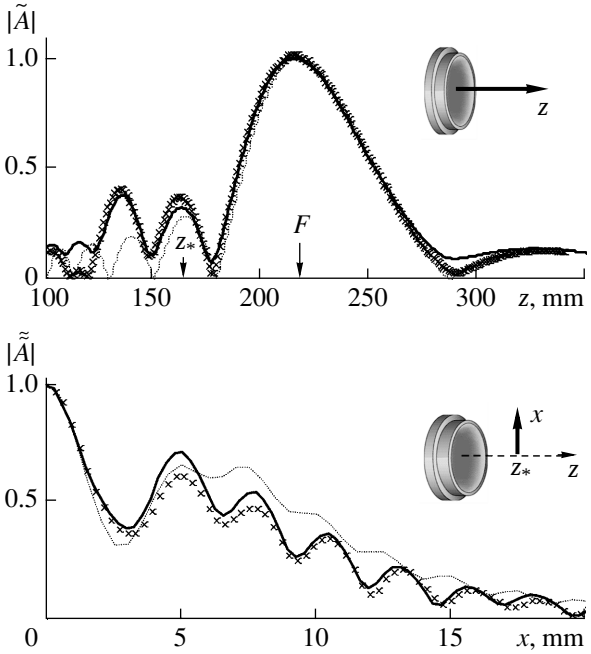

Fig. 7. Measured and calculated acoustic pressure. The upper panel shows the normalized pressure amplitude $|\tilde{A}| = |A|/A_F$ along the transducer axis. The lower panel shows the normalized pressure amplitude $|\tilde{\tilde{A}}| = |A|/A_*$ versus x coordinate for $z = z_* = 165$ mm. Here, $A_F = A(z = F)$ and $A_* = A(z = z_*)$ are the acoustic pressure amplitudes at the focus and on the axis of the transducer at $z = z_*$, respectively. The measured values are indicated by oblique crosses. The solid lines are calculated using the normal particle velocity distribution over the transducer surface that was reconstructed from the pressure measurements at z_0 = 214 mm. The dotted line represents the calculations for a piston transducer.

tally can serve as an implicit validity test for the curves in Fig. 5. To this end, we performed additional measurements of the wave amplitude. The upper panel in Fig. 7 shows the acoustic pressure distribution measured along the transducer axis, and the lower panel, the pressure distribution measured along the normal to the axis at the distance z_0 = 165 mm from the transducer. The thick solid lines are calculated from the reconstructed particle velocity, and the oblique crosses show the experimental results. Note that these calculations used the distribution reconstructed from the pressure measured at a different distance (z_0 = 214 mm) from the transducer. For the sake of comparison, the dotted lines show the pressure reconstructed from the uniform distribution of the normal particle velocity over the transducer. One can see that the calculation based on the reconstructed velocity distribution describes the true field structure much better. Minor differences between the calculations and the experiment can be attributed to the violation of the axial symmetry of the field generated by the transducer (Fig. 4). As was noted above, this effect was ignored in our calculations.

The proposed method of reconstructing the velocity field was also applied to other transducers. The results were similar, which allows us to conclude that the method can be used to reconstruct the normal particle velocity on the surfaces of different transducers.

ACKNOWLEDGMENTS

This work was supported by the Russian Foundation for Basic Research (project nos. 02-02-16999 and 02-02-17029), by the CRDF (grant no. RP2-2384-MO-02), and by the NIH-Fogarty (grant no. R03-TW006150-01).

REFERENCES

1. A. D. Pierce, *Acoustics* (Acoust. Soc. Am., Woodbury, NY, 1989).
2. D. Cathignol, O. A. Sapozhnikov, and J. Zhang, J. Acoust. Soc. Am. **101**, 1286 (1997).
3. D. Cathignol, O. A. Sapozhnikov, and Y. Theillere, J. Acoust. Soc. Am. **105**, 2612 (1999).
4. M. Fink, Phys. Today **50**, 34 (1997).
5. X. Fan, E. G. Moros, and W. L. Straube, J. Acoust. Soc. Am. **102**, 2734 (1997).
6. E. G. Williams and J. D. Maynard, Phys. Rev. Lett. **45**, 554 (1980).
7. E. G. Williams, J. D. Maynard, and E. Skudrzyk, J. Acoust. Soc. Am. **68**, 340 (1980).
8. E. G. Williams, *Fourier Acoustics: Sound Radiation and NAH* (Academic, London, 1999).
9. P. R. Stepanishen and K. C. Benjamin, J. Acoust. Soc. Am. **71**, 803 (1982).
10. M. E. Schafer and P. A. Lewin, J. Acoust. Soc. Am. **85**, 2202 (1989).
11. G. T. Clement and K. Hyhynen, J. Acoust. Soc. Am. **108**, 441 (2000).
12. E. L. Shenderov, *Emission and Scattering of Sound* (Sudostroenie, Leningrad, 1989).
13. D. Cathignol and O. A. Sapozhnikov, Akust. Zh. **45**, 816 (1999) [Acoust. Phys. **45**, 735 (1999)].

Translated by A. Khzmalyan